SUPPLEMENTARY MATERIALS AND METHODS

Stability Analysis of the System of Differential Equations

The model for yolk utilization over time given in Eqn (3) describes a decreasing logistic curve for the yolk area and therefore can be rewritten, given by Eqn (S1).

$$\frac{dY}{dt} = -cY\left(1 - \frac{Y}{k_1}\right) \qquad \text{(S1)}$$

Fixed points (i.e. steady state) for the system are found by setting $\frac{dy}{dt} = 0$ and solving for y. We see that the two steady states (SS) for the system are then $SS1 = 0, SS2 = k_1$. Algebraic stability analysis reveals SS1 is stable and SS2 is unstable (Murray, 2007). The stability of SS1 implies yolk area will ultimately be depleted, falling in line with the biological assumption.

The dynamic model for length over time is given by Eqn (S2), an increasing logistic curve.

$$\frac{dL}{dt} = dL\left(1 - \frac{L}{k_2}\right) \qquad \text{(S2)}$$

In the same manner as the preceding description, we determine two steady states $SS1 = 0, SS2 = k_2$. Algebraic stability analysis reveals SS1 is unstable while SS2 is stable. We conclude that upon ultimate time, the fish length will reach its maximum length k_2.

The system of two ordinary differential equations describing the interaction between yolk utilization and fish length growth are given by Eqn 11. The equilibrium points E^0 and E^* for the system of differential equations are found by determining where both $\frac{dY}{dt}$ and $\frac{dL}{dt}$ are both zero. That is,

$$E^0 = (Y^0, L^0) = (0,0)\,,$$

$$E^* = (Y^*, L^*) = \left(\frac{K_1\alpha + K_1K_2\beta}{\beta K_2}, K_2\right)$$

We notice E^0 is a nonphysical fixed point because it is biologically impossible for the fish length to be zero, therefore we eliminate the need to determine its stability. To determine the stability of E^*, we perform a linear stability analysis in which the Jacobian matrix is found and evaluated at the equilibrium point (Murray, 2007). The Jacobian J is calculated and evaluated at the steady state in order to calculate the eigenvalues and determine the stability of the steady state.

$$J = \begin{bmatrix} \frac{\partial Y}{\partial Y} & \frac{\partial L}{\partial Y} \\ \frac{\partial L}{\partial Y} & \frac{\partial L}{\partial L} \end{bmatrix} = \begin{bmatrix} \beta l \left(\frac{Y}{K_1} - 1\right) - \alpha + \frac{\beta}{K_1} LY & \beta Y \left(\frac{Y}{K_1} - 1\right) \\ -\gamma L \left(\frac{L}{K_2} - 1\right) & -\gamma L \left(\frac{L}{K_2} - 1\right) - \frac{\gamma}{K_2} LY \end{bmatrix}$$

At steady state E^* we obtain that

$$J|_{E^*} = \begin{bmatrix} \alpha + \beta K_2 & \frac{\alpha K_1(\alpha + \beta K_2)}{\beta K_2^2} \\ 0 & \frac{\gamma K_1(\alpha + \beta K_2)}{\beta K_2} \end{bmatrix}$$

The eigenvalues of the matrix $eig(J|_{E^*})$:

$$eig(J|_{E^*}) = [\lambda_1, \lambda_2] = \left[\alpha + \beta K_2, -\frac{\gamma K_1(\alpha + \beta K_2)}{\beta K_2}\right]$$

determine the stability of the steady state. Based on the expression $eig(J|_{E^*})$, we conclude that for any positive model parameter, E^* will be an unstable saddle node ($\lambda_1 > 0, \lambda_2 < 0$) (Keener and Sneyd, 1998; Murray, 2007). A solution trajectory for the coupled ordinary differential equation model is given in Fig. S6 along with a direction field to describe the behavior of all solution trajectories within close proximity of the unstable fixed point. As the arrows demonstrate, any solution will travel away from the fixed point and travel along the steady state solution to each equation in the coupled model.

Testing the Applicability of our Mathematical Model to an Environmental Condition

Toxicological manipulations of the developmental environment are commonly shown to change yolk use and fish growth at discrete timepoints. To gain an understanding of model adaptability to various developmental environments, zebrafish were exposed to an environmental pollutant, perfluorooctanesulfonic acid (PFOS (32 μM); CAS# 1763-23-1). Several studies have shown that PFOS disrupts yolk utilization in 4 dpf eleutheroembryos (Jantzen et al., 2016; Sant et al., 2017; Sant et al., 2018), but fish length is not significantly affected at the selected concentration (Sant et al., 2017; Sant et al., 2018). The independence of these variables allowed us to assess the robustness of our model. These previous works indicated that this concentration of PFOS did not increase mortality and the incidence of structural defects such as edema that could compromise the yolk measurements.

We conducted an assessment of yolk utilization and growth daily over the developmental period (1-5 dpf). Embryos were collected from 6 breeding tanks, fertilization was confirmed, and embryos were maintained in 0.3X Danieau's medium overnight in an incubator at 28.5°C. At 24 hpf, embryos were manually dechorionated using watchmakers' forceps, randomized,

and transferred to 100 mm polystyrene petri dishes. These embryos were then assigned to an exposure group: Control (0.01% *v/v* DMSO) or PFOS (32 μM). Similarly to control conditions, 30 ml of exposure media was added to each dish, and exposures were refreshed daily. DMSO was used as a vehicle for PFOS to ensure solubility in water. All microscopy procedures were performed daily as presented in the Methods section although the time frame for this investigation was 1-5 dpf. These experiments were repeated 4 times, each with 6-15 embryos per group (n=43 embryos in total per group).

There was no significant increase in heterogeneity (variance) due to exposures (Levene's test; p-value>0.05) and the mathematical model (Eqn. 11) still fit the yolk and fish length data (R^2 = 0.99, Fig. S7). The increased rate of yolk utilization is visible as an increased rate of change between 3.5-5.0 dpf (i.e., compared to controls), and decreased rate of change between 1.0-3.5dpf. The average increase in yolk utilization is obvious from the increase in the rate parameters α and β (Table S9) and is described in greater detail in the manuscript Results section "Testing the Applicability of our Model to an Environmental Condition."

Area as an Approximation for Yolk Volume

It is known that at the early stages of development the yolk is distorted on the 2D plane as there is significant depth to the yolk ball not seen in the image. This is most prominent at the early stages of development when the yolk may be viewed as a combination of an ellipsoid and a cylindrical tube. It is a concern that the 2D area measurement at this stage may incorrectly portray total yolk mass. To address this concern, we assessed the correlation of yolk area and volume between 2-3 dpf when the yolk is most distorted on a 2D plane. Images from a new control experiment were obtained using the same methodology used in this study. In addition to the sagittal images used in the original analysis, an additional image was captured where the fish was positioned on its back which displayed the depth of the yolk (Fig. S8A and B). Yolk volume measurements were computed for this data set (n=14) and yolk area measurements were also taken. That is, yolk volume V was computed as the sum of geometric shapes and the 2D area was found using the same method used throughout the study and described in Methods. Geometric shapes used include an ellipsoid ($V = 4\pi abc/3$ where a, b, c are the radii of the principal axes) and a cylinder *($V = \pi r^2 h$* where r is the radius and h is the height) (Fig. S8A and B). We then used regression to assess the implications of this distortion between 2 and 3 dpf, when the "tube" structure may have the biggest impact on the area. Statistical analyses show that there is a strong association between yolk volume and yolk area *(R^2 >0.85, p<0.01, FigS8C).* The short analyses conducted here shows that yolk volume and yolk area are positively correlated between 2-3 dpf when the yolk has a significant depth not captured by a 2D image. From this, we state that 2D modeling of the yolk, while not perfect, is an acceptable proxy for yolk volume in this study.

SUPPLEMENTAL DATA

Table S1. Yolk size measured by the total area in mm^2 covered by the yolk in the microscopy image

Original Yolk Size in mm^2							
Sample #	**Day 1**	**Day 2**	**Day 3**	**Day 4**	**Day 5**	**Day 6**	**Day 7**
1	3.19×10^{-1}	2.74×10^{-1}	2.09×10^{-1}	9.18×10^{-2}	1.98×10^{-2}	0	0
2	3.16×10^{-1}	2.67×10^{-1}	2.23×10^{-1}	7.87×10^{-2}	1.22×10^{-2}	0	0
3	3.36×10^{-1}	2.87×10^{-1}	2.36×10^{-1}	1.20×10^{-1}	1.69×10^{-2}	4.28×10^{-3}	0
4	3.14×10^{-1}	2.78×10^{-1}	2.34×10^{-1}	1.01×10^{-1}	1.43×10^{-2}	0	0
5	3.67×10^{-1}	2.71×10^{-1}	2.04×10^{-1}	4.62×10^{-2}	1.23×10^{-2}	2.18×10^{-3}	0
6	3.32×10^{-1}	3.05×10^{-1}	2.34×10^{-1}	1.07×10^{-1}	1.61×10^{-2}	0	0
7	3.77×10^{-1}	3.08×10^{-1}	2.21×10^{-1}	1.47×10^{-1}	1.95×10^{-2}	5.15×10^{-3}	0
8	3.32×10^{-1}	2.98×10^{-1}	2.25×10^{-1}	1.10×10^{-1}	1.57×10^{-2}	5.92×10^{-3}	0
9	2.71×10^{-1}	2.13×10^{-1}	1.50×10^{-1}	7.54×10^{-2}	4.54×10^{-3}	1.83×10^{-3}	0
10	3.23×10^{-1}	2.95×10^{-1}	2.11×10^{-1}	6.89×10^{-2}	9.35×10^{-3}	3.83×10^{-3}	0
11	3.40×10^{-1}	2.76×10^{-1}	2.33×10^{-1}	6.85×10^{-2}	8.44×10^{-3}	5.95×10^{-3}	0
12	3.32×10^{-1}	2.69×10^{-1}	2.17×10^{-1}	8.59×10^{-2}	6.58×10^{-3}	1.25×10^{-2}	0
13	3.77×10^{-1}	2.85×10^{-1}	2.46×10^{-1}	1.49×10^{-1}	1.08×10^{-2}	2.12×10^{-3}	0
14	3.38×10^{-1}	3.11×10^{-1}	2.48×10^{-1}	1.84×10^{-1}	1.64×10^{-2}	5.90×10^{-3}	0

Table S2. Fish length from the beginning of the spine to the end of the tail measured in mm

Original Length Data in mm							
Sample #	**Day 1**	**Day 2**	**Day 3**	**Day 4**	**Day 5**	**Day 6**	**Day 7**
1	1.62	2.86	3.04	3.47	3.35	3.51	3.44
2	1.67	3.01	3.30	3.64	3.77	3.76	3.79
3	2.00	3.16	3.41	3.65	3.84	3.84	3.82
4	1.87	3.10	3.38	3.68	3.82	3.81	3.77
5	2.07	3.15	3.43	3.71	3.76	3.79	3.78
6	2.07	3.25	3.51	3.87	4.00	3.96	3.82
7	1.84	3.19	3.46	3.71	3.87	3.86	3.72
8	2.07	3.13	3.29	3.68	3.82	3.78	3.80
9	1.86	3.00	3.25	3.45	3.46	3.47	3.44
10	1.90	3.09	3.33	3.68	3.76	3.74	3.75
11	1.90	3.20	3.49	3.75	3.93	3.91	3.93
12	2.20	3.27	3.54	3.85	4.01	3.96	3.96
13	2.05	3.24	3.50	3.80	4.06	3.96	3.98
14	1.83	3.12	3.46	3.80	4.05	3.97	3.93

Table S3. Normalized yolk size, computed from Table S1

Normalized Yolk Size							
Sample #	**Day 1**	**Day 2**	**Day 3**	**Day 4**	**Day 5**	**Day 6**	**Day 7**
1	8.46×10^{-1}	7.27×10^{-1}	5.55×10^{-1}	2.44×10^{-1}	5.26×10^{-2}	0	0
2	8.39×10^{-1}	7.08×10^{-1}	5.92×10^{-1}	2.09×10^{-1}	3.25×10^{-2}	0	0
3	8.90×10^{-1}	7.61×10^{-1}	6.26×10^{-1}	3.19×10^{-1}	4.49×10^{-2}	1.14×10^{-2}	0
4	8.33×10^{-1}	7.37×10^{-1}	6.21×10^{-1}	2.67×10^{-1}	3.78×10^{-2}	0	0
5	9.73×10^{-1}	7.18×10^{-1}	5.40×10^{-1}	1.23×10^{-1}	3.26×10^{-2}	5.78×10^{-3}	0
6	8.80×10^{-1}	8.10×10^{-1}	6.22×10^{-1}	2.85×10^{-1}	4.27×10^{-2}	0	0
7	9.99×10^{-1}	8.16×10^{-1}	5.87×10^{-1}	3.90×10^{-1}	5.18×10^{-2}	1.37×10^{-2}	0
8	8.80×10^{-1}	7.91×10^{-1}	5.97×10^{-1}	2.92×10^{-1}	4.15×10^{-2}	1.57×10^{-2}	0
9	7.19×10^{-1}	5.65×10^{-1}	3.98×10^{-1}	2.00×10^{-1}	1.21×10^{-2}	4.86×10^{-3}	0
10	8.56×10^{-1}	7.81×10^{-1}	5.58×10^{-1}	1.83×10^{-1}	2.48×10^{-2}	1.02×10^{-2}	0
11	9.02×10^{-1}	7.31×10^{-1}	6.18×10^{-1}	1.82×10^{-1}	2.24×10^{-2}	1.58×10^{-2}	0
12	8.82×10^{-1}	7.14×10^{-1}	5.75×10^{-1}	2.28×10^{-1}	1.75×10^{-2}	3.31×10^{-2}	0
13	1	7.56×10^{-1}	6.53×10^{-1}	3.96×10^{-1}	2.87×10^{-2}	5.62×10^{-3}	0
14	8.96×10^{-1}	8.24×10^{-1}	6.58×10^{-1}	4.89×10^{-1}	4.36×10^{-2}	1.57×10^{-2}	0

Table S4. Normalized fish length, computed from Table S2

Normalized Length Data							
Sample #	**Day 1**	**Day 2**	**Day 3**	**Day 4**	**Day 5**	**Day 6**	**Day 7**
1	4.07×10^{-1}	7.19×10^{-1}	7.63×10^{-1}	8.73×10^{-1}	8.41×10^{-1}	8.81×10^{-1}	8.65×10^{-1}
2	4.21×10^{-1}	7.55×10^{-1}	8.28×10^{-1}	9.13×10^{-1}	9.48×10^{-1}	9.43×10^{-1}	9.51×10^{-1}
3	5.02×10^{-1}	7.95×10^{-1}	8.56×10^{-1}	9.16×10^{-1}	9.66×10^{-1}	9.66×10^{-1}	9.59×10^{-1}
4	4.70×10^{-1}	7.79×10^{-1}	8.48×10^{-1}	9.22×10^{-1}	9.60×10^{-1}	9.58×10^{-1}	9.47×10^{-1}
5	5.19×10^{-1}	7.90×10^{-1}	8.61×10^{-1}	9.31×10^{-1}	9.45×10^{-1}	9.52×10^{-1}	9.50×10^{-1}
6	5.21×10^{-1}	8.15×10^{-1}	8.83×10^{-1}	9.71×10^{-1}	1.01	9.95×10^{-1}	9.61×10^{-1}
7	4.61×10^{-1}	8.02×10^{-1}	8.70×10^{-1}	9.32×10^{-1}	9.73×10^{-1}	9.72×10^{-1}	9.35×10^{-1}
8	5.19×10^{-1}	7.86×10^{-1}	8.27×10^{-1}	9.26×10^{-1}	9.61×10^{-1}	9.52×10^{-1}	9.54×10^{-1}
9	4.68×10^{-1}	7.53×10^{-1}	8.16×10^{-1}	8.68×10^{-1}	8.68×10^{-1}	8.72×10^{-1}	8.64×10^{-1}
10	4.79×10^{-1}	7.75×10^{-1}	8.38×10^{-1}	9.24×10^{-1}	9.45×10^{-1}	9.40×10^{-1}	9.42×10^{-1}
11	4.77×10^{-1}	8.04×10^{-1}	8.76×10^{-1}	9.43×10^{-1}	9.87×10^{-1}	9.82×10^{-1}	9.87×10^{-1}
12	5.53×10^{-1}	8.22×10^{-1}	8.90×10^{-1}	9.68×10^{-1}	1.01	9.94×10^{-1}	9.95×10^{-1}
13	5.15×10^{-1}	8.15×10^{-1}	8.80×10^{-1}	9.56×10^{-1}	1.02	9.94×10^{-1}	1
14	4.6×10^{-1}	7.84×10^{-1}	8.69×10^{-1}	9.53×10^{-1}	1.02	9.97×10^{-1}	9.88×10^{-1}

Table S5. Computed parameter values for the different models for yolk absorption

Parameter Estimations for the different models					
	Exponential Model	**Hill's Function**		**Logistic Model**	
Sample #	a	b_1	n_1	k_1	c
1	3.89×10^{-1}	3.32	5.38	8.74×10^{-1}	1.46
2	3.94×10^{-1}	3.36	6.38	8.53×10^{-1}	1.71
3	3.68×10^{-1}	3.47	5.57	9.14×10^{-1}	1.46
4	3.66×10^{-1}	3.51	6.64	8.42×10^{-1}	1.75
5	4.79×10^{-1}	2.86	4.44	1.05	1.36
6	3.67×10^{-1}	3.46	6.25	8.93×10^{-1}	1.68
7	3.88×10^{-1}	3.24	4.25	1.08	1.12
8	3.71×10^{-1}	3.42	5.68	9.01×10^{-1}	1.53
9	4.34×10^{-1}	3.03	4.34	7.86×10^{-1}	1.22
10	4.01×10^{-1}	3.27	6.61	8.67×10^{-1}	1.87
11	4.13×10^{-1}	3.27	6.23	9.21×10^{-1}	1.70
12	4.06×10^{-1}	3.23	5.16	9.18×10^{-1}	1.44
13	3.89×10^{-1}	3.30	4.34	1.07	1.16
14	3.23×10^{-1}	3.81	6.20	9.07×10^{-1}	1.57

Table S6. Computed parameter values for the different models for fish growth

Parameter Estimations for the different models for				
	Hill's Function		Logistic Model	
Sample #	b_2	n_2	k_2	d
1	1.05	2.45	8.67×10^{-1}	1.16
2	1.11	2.28	9.46×10^{-1}	1.14
3	9.64×10^{-1}	2.17	9.53×10^{-1}	1.36
4	1.02	2.33	9.49×10^{-1}	1.29
5	9.27×10^{-1}	2.19	9.44×10^{-1}	1.43
6	9.46×10^{-1}	2.55	9.81×10^{-1}	1.44
7	1.02	2.80	9.51×10^{-1}	1.48
8	9.26×10^{-1}	2.03	9.49×10^{-1}	1.26
9	9.44×10^{-1}	2.68	8.66×10^{-1}	1.57
10	9.93×10^{-1}	2.25	9.39×10^{-1}	1.30
11	1.03	2.23	9.76×10^{-1}	1.35
12	9.11×10^{-1}	2.10	9.90×10^{-1}	1.43
13	9.83×10^{-1}	2.13	9.94×10^{-1}	1.33
14	1.08	2.31	9.96×10^{-1}	1.18

Table S7. Computed parameters for the system of differential equations

Parameter estimates					
Sample #	α	β	γ	K_1	K_2
1	5.59×10^{-2}	1.65	1.78	8.51×10^{-1}	8.87×10^{-1}
2	3.05×10^{-2}	1.79	1.61	8.50×10^{-1}	9.86×10^{-1}
3	3.86×10^{-2}	1.51	1.39	9.00×10^{-1}	9.93×10^{-1}
4	1.90×10^{-2}	1.84	1.56	8.40×10^{-1}	9.82×10^{-1}
5	9.51×10^{-2}	1.38	1.16	1.02	1.04
6	3.26×10^{-2}	1.71	1.40	8.80×10^{-1}	1.02
7	1.08×10^{-1}	1.09	1.62	9.94×10^{-1}	9.73×10^{-1}
8	4.63×10^{-2}	1.61	1.17	8.80×10^{-1}	1.02
9	1.08×10^{-1}	1.30	2.32	7.31×10^{-1}	8.86×10^{-1}
10	4.30×10^{-2}	1.99	1.48	8.50×10^{-1}	9.86×10^{-1}
11	4.99×10^{-2}	1.72	1.45	9.03×10^{-1}	1.03
12	7.34×10^{-2}	1.42	1.17	8.80×10^{-1}	1.08
13	9.58×10^{-2}	1.11	1.12	1.00	1.07
14	1.85×10^{-2}	1.60	1.34	9.02×10^{-1}	1.03

Table S8. Degree of variation in computed parameters

	Parameter	**% within one standard deviation**
Yolk logistic model	k_1	92.86
	a	78.57
Length logistic model	k_2	71.43
	d	64.29
System of ODE	α	57.14
	β	71.43
	γ	85.71
	K_1	71.43
	K_2	71.43

Table S9. Mean parameter values for the PFOS investigation

Parameter	Control	32 μM PFOS
α	1.03×10^{-2}	1.9×10^{-2}
β	1.95	2.95
γ	2.57	2.54
K_1	0.92	0.91
K_2	0.86	0.86

SUPPLEMENTAL FIGURES

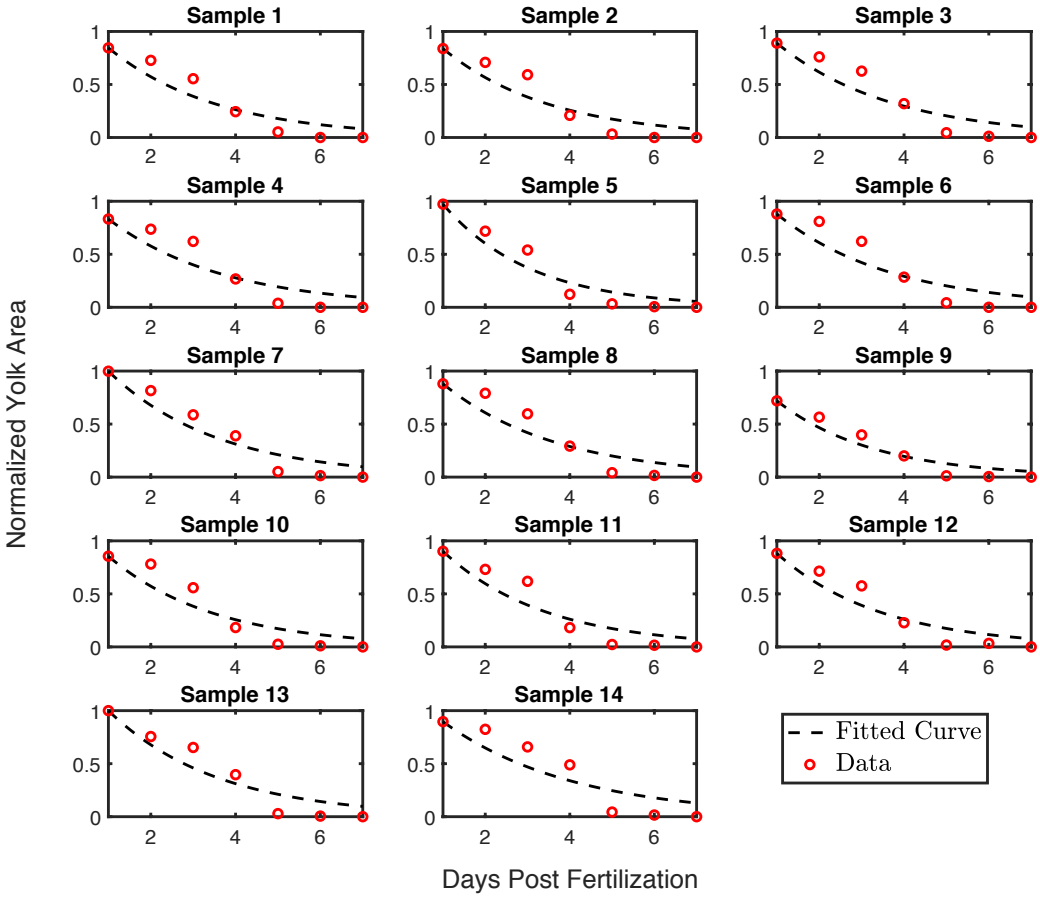

Figure S1. Exponential fit of normalized yolk over time for individual fish samples. y-axis represents the yolk area; x-axis represents age in days post fertilization (dpf).

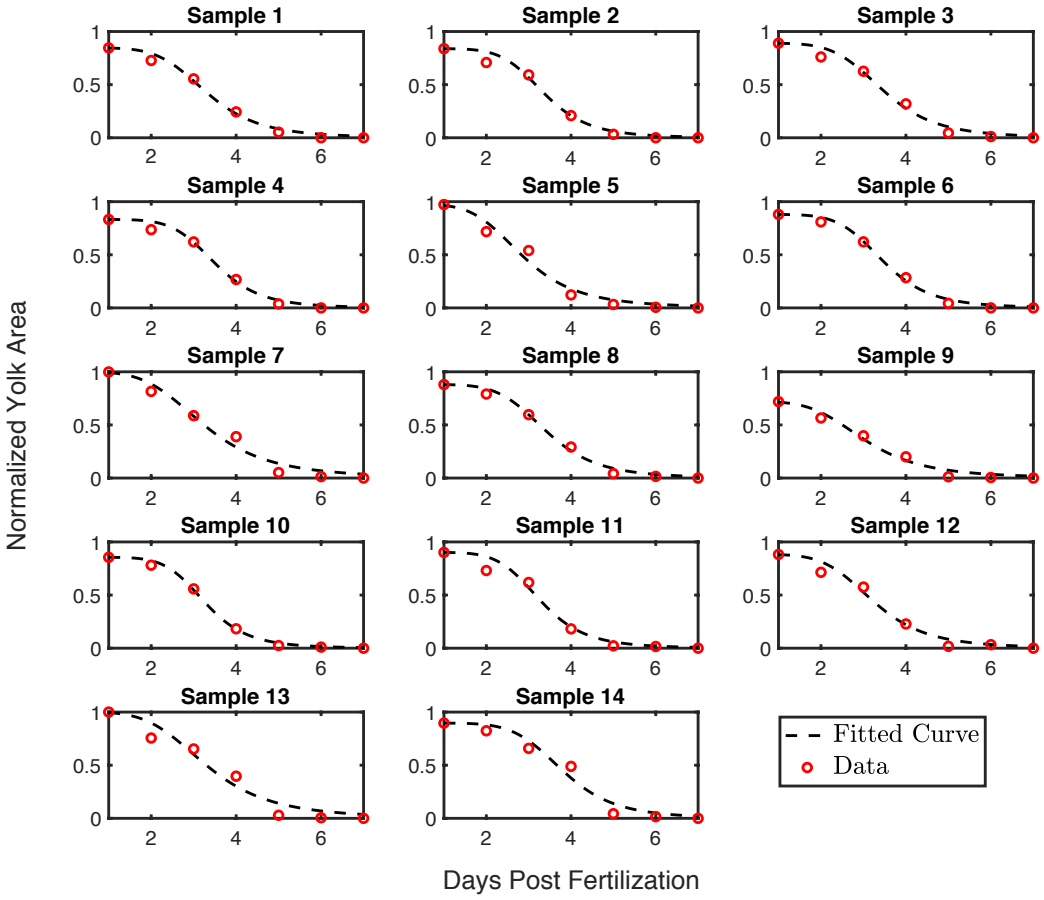

Figure S2. Hill's function fit of normalized yolk over time for individual fish samples. y-axis represents normalized yolk area; x-axis represents the age in dpf.

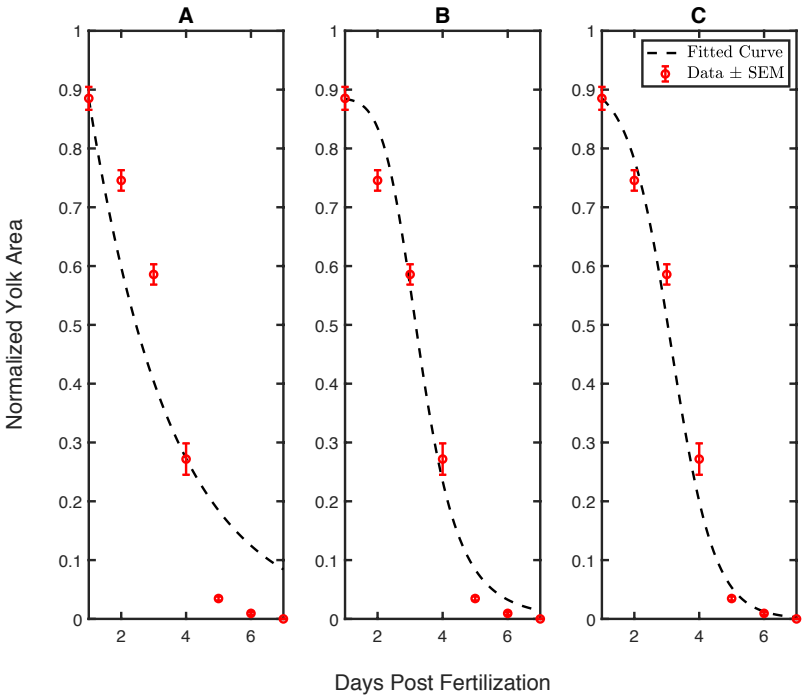

Figure S3. Plots of the mean normalized data for yolk area ± standard error from the mean along with the best-fit curves for the exponential function (A), Hill's function (B), and the logistic function (C). y-axis represents the normalized yolk area; x-axis represents the age in dpf.

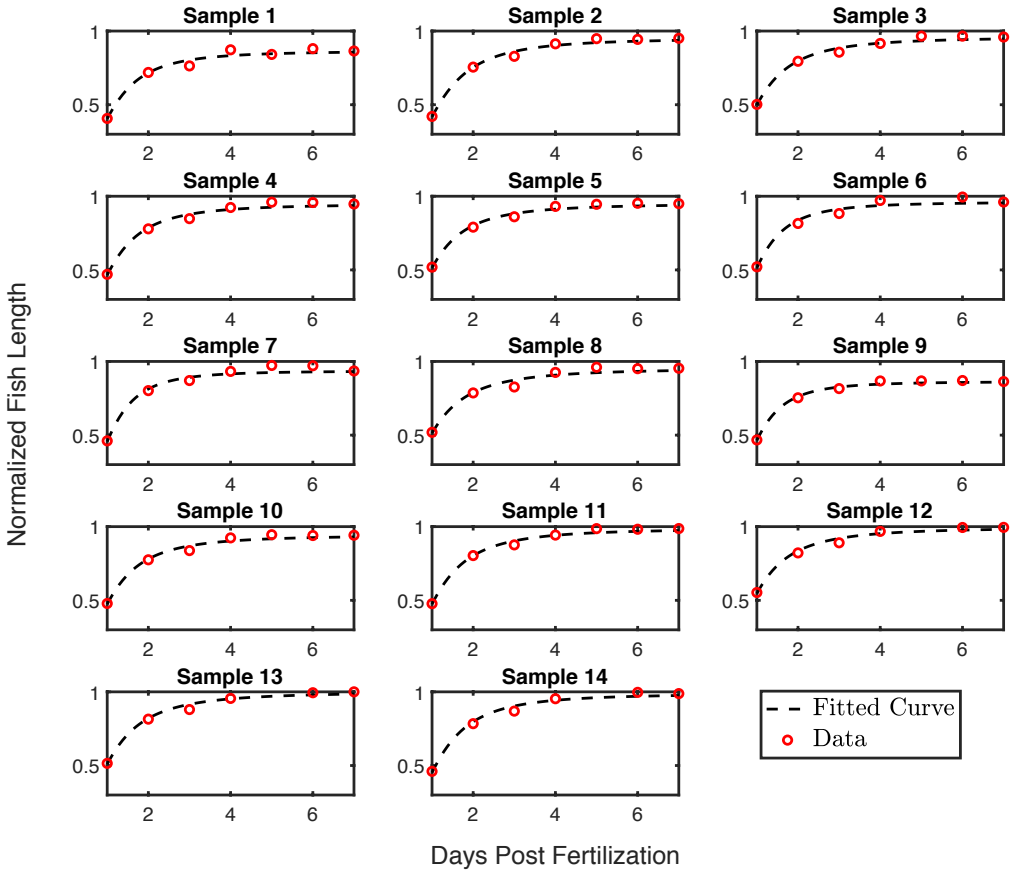

Figure S4. Hill's function fit of normalized fish length over time. y-axis represents the fish length; x-axis represents the age in dpf.

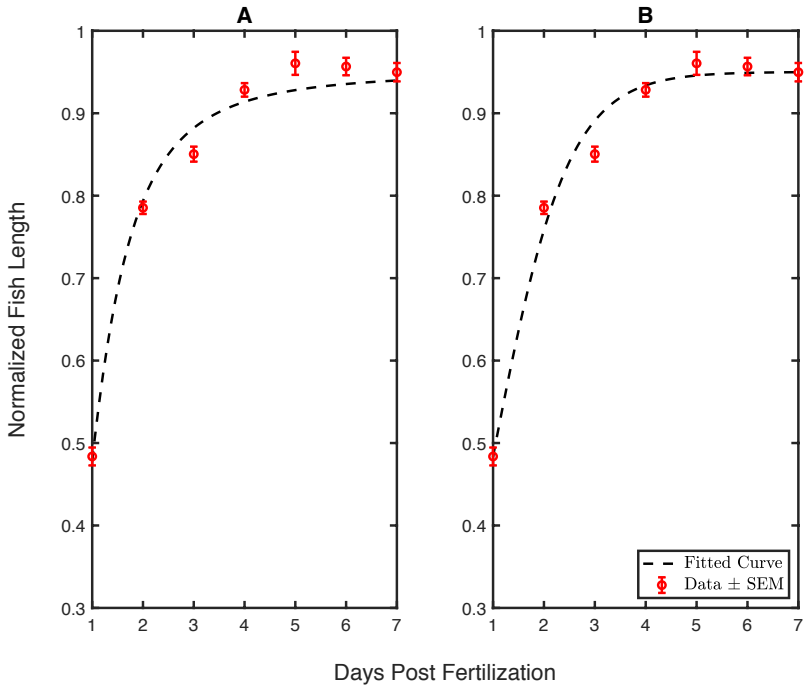

Figure S5. Plots of the mean normalized data for fish length ± standard error from the mean along with the best-fit curves for Hill's function (A) and the logistic function (B).

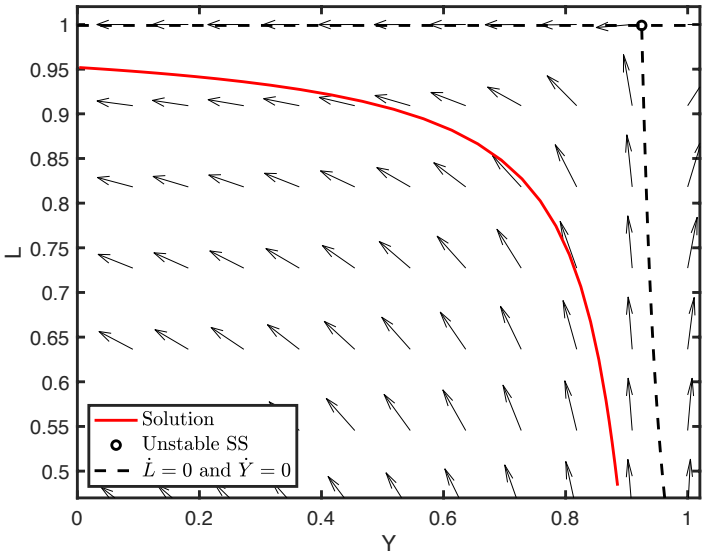

Figure S6. A phase plane of the coupled ordinary differential equation model displaying a solution trajectory (red line) traveling away from the unstable steady state (open bullet) along the nullclines for the model (dashed lines) in the direction of the arrows.

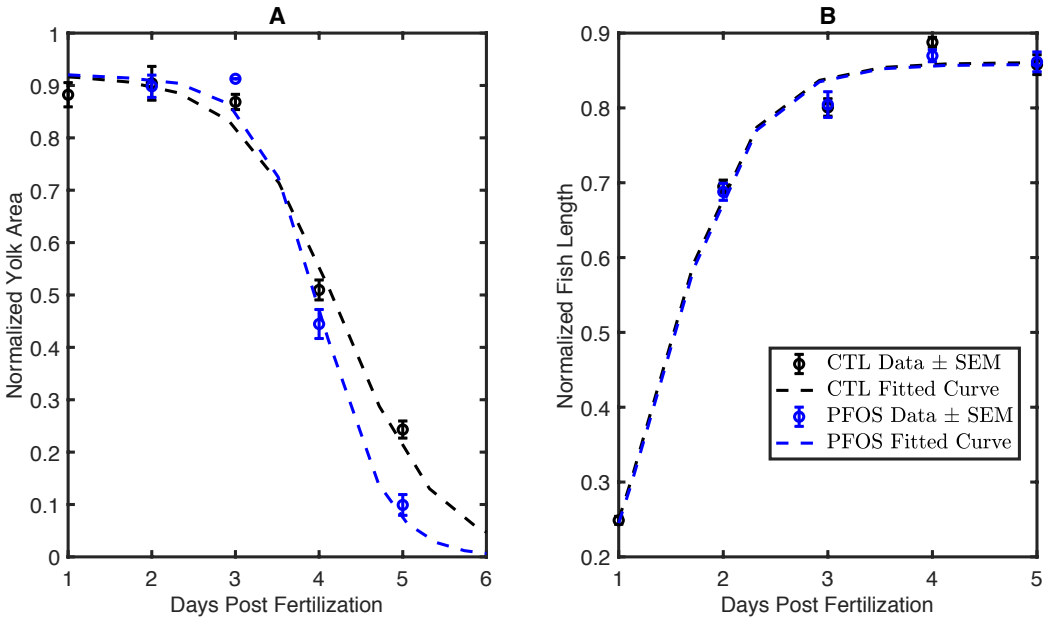

Figure S7. Toxicological perturbation during the embryonic and larval periods due to PFOS exposures increases the rate of yolk utilization but the mathematical models (Eqn. 11) still fits the data for yolk area over time (A) and fish length over time (B) (R^2 = 0.99). Data were obtained from four experiments, using embryos randomized from six breeding tanks. n=43 per group.

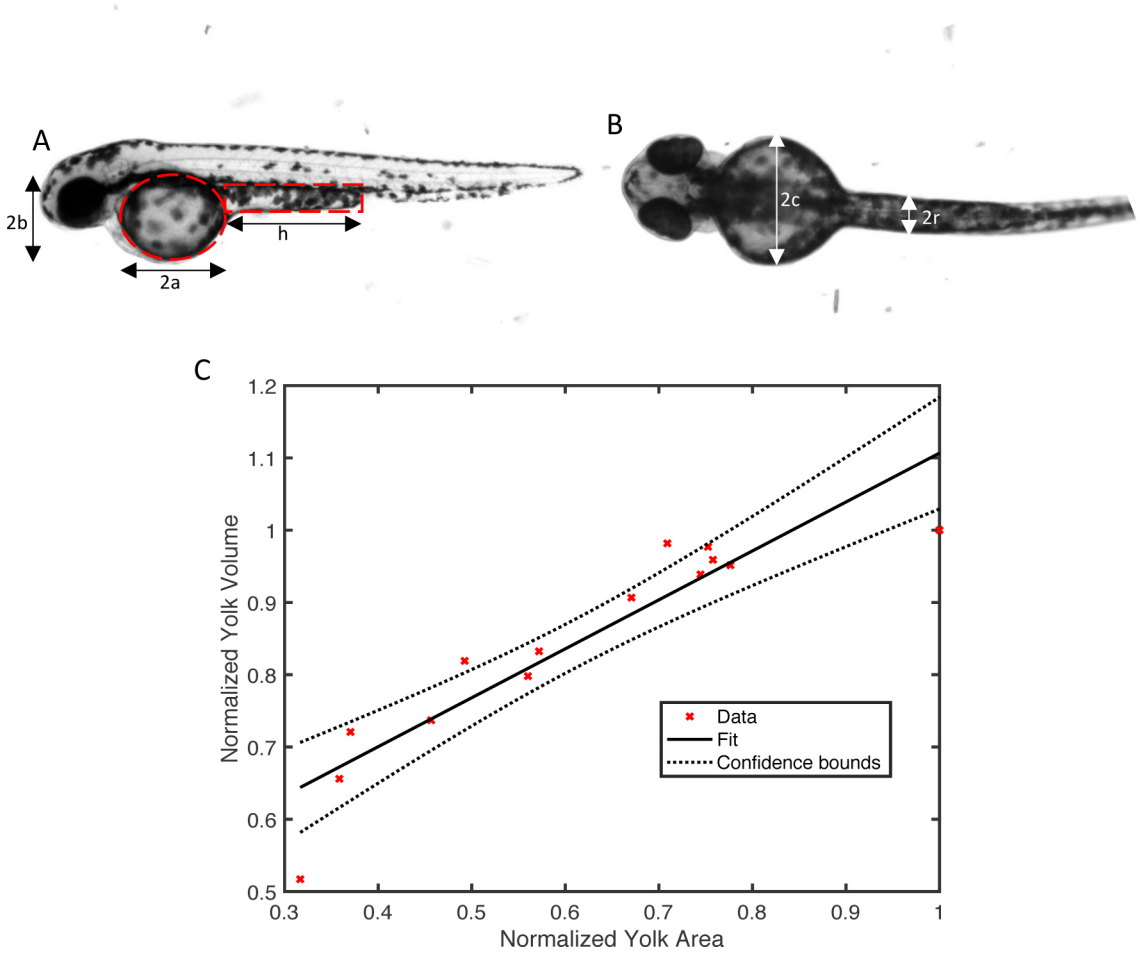

Figure S8. Correlation between normalized yolk area and normalized yolk volume at 2-3 dpf. (A) Sagittal plane image of zebrafish used to compute the yolk area. (B) Coronal plane image of zebrafish used to compute the size of yolk in the z plane. Measurements taken from Fig. A and B is used to compute the yolk volume. Statistical analysis reveals a strong association ($R^2 > 0.85$, $p < 0.01$), n=14 zebrafish embryos. Best fit line is: $y = 0.68x + 0.43$, where y and x represent the normalized yolk volume and normalized yolk area respectively.

SUPPLEMENTAL REFERENCES

Jantzen, C.E., Annunziato, K.A., Bugel, S.M., Cooper, K.R., 2016. PFOS, PFNA, and PFOA sub-lethal exposure to embryonic zebrafish have different toxicity profiles in terms of morphometrics, behavior and gene expression. Aquat Toxicol 175, 160-170.
Keener, J.P., Sneyd, J., 1998. Mathematical physiology. Springer.
Murray, J.D., 2007. Mathematical biology: I. An introduction. Springer Science & Business Media.
Sant, K.E., Jacobs, H.M., Borofski, K.A., Chen, P., Park, Y., Timme-Laragy, A.R., 2017. Pancreas Development and Nutrient Uptake and Utilization Are Disrupted by Embryonic Exposures to the Environmental Toxicant Perfluorooctanesulfonic Acid in the Zebrafish. The FASEB Journal 31, 792-8.
Sant, K.E., Sinno, P.P., Jacobs, H.M., Timme-Laragy, A.R., 2018. Nrf2a modulates the embryonic antioxidant response to perfluorooctanesulfonic acid (PFOS) in the zebrafish, Danio rerio. Aquatic Toxicology 198, 92-102.